JOURNAL OF GEOPHYSICAL RESEARCH, VOL. 95, NO. A5, PAGES 6467-6475, MAY 1, 1990

OBSERVATIONS AND MODELING OF WAVE-INDUCED MICROBURST ELECTRON PRECIPITATION

T. J. Rosenberg, R. Wei[1] and D. L. Detrick

Institute for Physical Science and Technology, University of Maryland at College Park

U. S. Inan

STARLaboratory, Stanford University, Stanford, California

Abstract. Energy-time features of X ray microbursts are examined and compared with the predictions of a test particle simulation model of wave-induced electron precipitation resulting from gyroresonant wave-particle interactions in the magnetosphere. The observations were obtained on a balloon flight at Siple station, Antarctica (L ≈ 4.2) on December 30, 1980. The energy and time evolution of the microbursts were studied for X rays in the energy range from 25 to 175 keV. An algorithm designed to search the E > 25 keV counting rate data for single isolated microbursts identified 651 events in a 3-hr interval. The distribution of burst durations ranged from 0.2 to 1.2 s. Approximately two-thirds of the distribution were narrow bursts (0.2-0.6 s), the rest wide (0.6-1.2 s), with the average burst durations equal to ~ 0.4 s and ~ 0.7 s, respectively, for the two classes. The precipitation was characterized by exponential electron spectra with e-folding energies Eo of 25-50 keV. Individual and superposed microburst profiles show that the X ray energy spectrum is softest (equivalent to a reduction in electron Eo of ≤ 5 keV) near the peak of the energy influx. Computer simulations of the flux- and energy-time profiles of direct and mirrored electron precipitation induced by a whistler-mode wave pulse of 0.2-s duration and linear frequency increase from 2 to 4 kHz were performed for plasma, energetic particle and wave parameters appropriate for the location and geophysical conditions of the observations. The wave pulse is representative of the VLF chorus elements that were observed at Siple station and at the conjugate location of Roberval, Quebec during the microburst activity on this day. In both the direct and mirrored cases the combined effect of latitude dependence of the energy of maximum gyroresonant scattering and energy dispersion leads to energy spectrum variations qualitatively consistent with the microburst observations. The average burst durations in the two cases were ~ 0.3 s (direct) and ~ 0.7 s (mirrored). On this basis we identify the narrow microbursts with electrons which are precipitated directly after undergoing pitch-angle scattering interactions with the wave pulse; the wide microbursts are identified with electrons which, after interacting with the wave, mirror in the conjugate ionosphere before precipitating into the southern ionosphere. In general, the results provide further support for the gyroresonant test particle simulation model, and for the belief that the observed type of microbursts originates in the vicinity of the magnetic equator in a gyroresonant process involving discrete chorus emissions.

Introduction

The pitch-angle scattering incurred by radiation belt electrons in cyclotron resonance with magnetospheric whistler-mode waves has long been considered one of the principal mechanisms for precipitating energetic electrons into the atmosphere [e.g., Kennel and Petschek, 1966]. Such interactions, for example, are thought to account for lightning-induced precipitation [Bering et al., 1980; Voss et al., 1984; Chang and Inan, 1985a; Inan et al., 1985; Goldberg et al., 1986] and precipitation stimulated artificially by VLF transmitters [Imhof et al., 1983].

One of the most striking examples of a precipitation structure that is probably caused by gyroresonant wave-particle interaction is the microburst [Anderson and Milton, 1964], an impulsive burst of electrons of ≤ 1-s duration that is associated with the occurrence of natural ELF/VLF chorus activity [Oliven and Gurnett, 1968; Roeder et al., 1985]. Evidence that microbursts are produced by electron pitch angle scattering in interactions with ELF/VLF waves is suggested by the high degree of correlation that is observed on occasion between individual microbursts (or microburst-like pulses) and chorus elements [Rosenberg et al., 1971, 1981; Foster and Rosenberg, 1976; Helliwell et al., 1980]. It has also been shown in the case of the latter four references, which pertain to measurements at L ≈ 4, and by Khrustchinsky et al. [1984], that microburst source regions lie within approximately 20° of the geomagnetic equator where the conditions for cyclotron resonance are readily satisfied by the observed electron energies and wave frequencies. Other measurements, particularly for L ≈ 6-8, have been interpreted as placing the microburst source region further from the equator along the field line [Anderson and Milton, 1964; Haugstad and Pytte, 1977], as well as near the ionosphere [Lampton, 1967].

Although a number of aspects of microburst electron precipitation have been examined in considerable detail (e.g., see reviews by Parks [1975, 1978] and Lazutin [1986]), there have been no studies of the energy spectra of microbursts at high time resolution during periods of correlated magnetospheric wave activity. Such studies are needed in order to further establish the physical basis of the microburst process.

---

[1]Presently at Institute of Space Physics, Chinese Academy of Sciences, Beijing.

Paper number 90JA00096.
0148-0227/90/90JA-00096$05.00

The intent of this paper is to characterize in detail the energy-time features of X ray microbursts and to compare the observed features with simulations of burst precipitation derived from a test particle computer model of the gyroresonance wave-particle interaction in the magnetosphere [Inan et al., 1978, 1982; Chang and Inan, 1983a; Chang et al, 1983]. Model computations are performed for a range of plasma, energetic particle, and wave parameters appropriate for the location and geophysical conditions of the observations. The model has been used by Chang and Inan [1983b] to confirm and extend the results presented in several earlier studies [Rosenberg et al., 1971; Helliwell et al., 1973, 1980] in which gyroresonance interactions were believed to be responsible for the burst precipitation of electrons on short ($\leq$ 1 s) time scales. The present work differs from that of Chang and Inan [1983b] in that the energy spectrum and time variations of the observed microbursts and the frequency-time characteristics of the accompanying VLF chorus activity are better defined, thus permitting a more detailed comparison with theoretical predictions than was previously possible.

Instrumentation

The microburst data used in this study were obtained by an X ray spectrometer on a balloon launched from Siple station, Antarctica (76° S; 84° W; L $\approx$ 4.2) on December 30, 1980. The detector was a 7.62 cm diameter by 1.27 cm thick NaI(Tl) scintillation counter that recorded the bremsstrahlung X rays produced in the upper atmosphere during the precipitation of energetic electrons. The geometric factor of the instrument (omnidirectional over the upper hemisphere) was 191 cm^2-sr. X ray counts were accumulated in 10-ms intervals in eight energy ranges extending from 25 keV to 500 keV; for the purpose of this study, 0.1-s averages of the counting rates were employed.

Continuous broadband (0-30 kHz) ELF/VLF recordings were also made on the ground at Siple station and at Roberval, Canada (48.50° N; 72.25° W), near the Siple conjugate point. The interhemispheric timing accuracy was maintained to within 10 ms.

Observations

A plot of the X ray counting rate in the 25-45 keV energy channel from near launch at ~ 0939 UT until the end of the day is given in Figure 1 of Gaines et al. [1986]. Here, in Figure 1, we show 1-min averages of the X ray counting rates in the > 25 keV and 125-175 keV energy channels for the early portion of the flight when microbursts were observed. During this interval of activity the balloon was within 50 km of the launch site. The balloon reached its stable float altitude of 8 g cm^{-2} at ~ 1100 UT. Dashed lines indicate the counting rate levels contributed by the cosmic-ray background at this atmospheric depth.

As shown in Figure 1, the most intense electron precipitation occurred around 1100 UT (0600 MLT); subsequent, weaker enhancements were centered about 1155 UT and 1245 UT. It is evident from comparing the relative enhancements in the two X ray energy channels that the energy

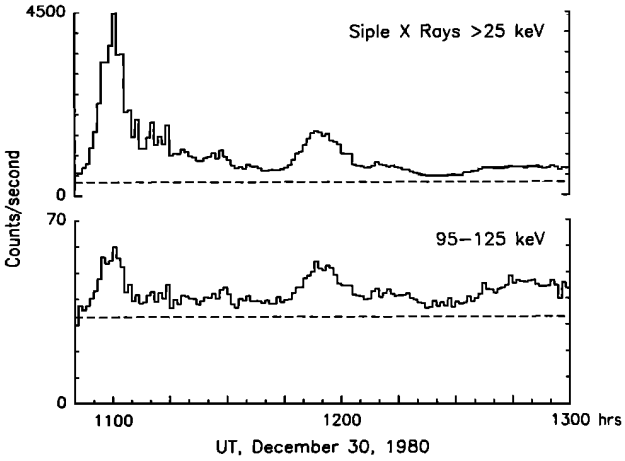

Fig. 1. X ray counting rates (1-min averages) in two energy ranges, E > 25 keV and 125 $\leq$ E $\leq$ 175 keV, for the period 1050-1300 UT when microbursts were observed. The data were obtained on a balloon flight from Siple station, Antarctica on December 30, 1980. The dashed lines are the background counting rates due to galactic cosmic rays.

spectrum of the precipitated electrons was softest during the initial activity, becoming increasingly harder throughout the rest of the time interval displayed.

A 30-s segment of the microburst/VLF wave activity recorded shortly after the balloon reached its ceiling altitude is shown in Figure 2. Three channels of X ray data (E > 25 keV, 25 < E $\leq$ 45 keV, and 45 < E $\leq$ 65 keV) at 0.1-s resolution are illustrated along with the 0- to 5-kHz wave spectrum recorded on the ground at Siple station and at Roberval. Prominent X ray bursts in the E > 25 keV panel are labeled N (narrow) and W (wide) referring to the burst duration; the precise definitions of N and W are discussed later. Other weaker bursts, although statistically significant, are more difficult to categorize in this simple way. Although most of the microbursts could be described as either narrow or wide, there was considerable diversity in the structures observed overall. Multiple overlapping and non-overlapping bursts and bursts with fast rise, slow decay and slow rise, fast decay were evident. This diversity of microburst types is consistent with previous observations.

Figure 2 also illustrates that a band of chorus with frequencies in the range of ~ 2 to 4 kHz occurred in the same time interval as the microbursts. Many more chorus elements than statistically significant microbursts are evident, however, which we attribute at least in part to the much larger field of view of the VLF receiver. Chorus in this frequency range has previously been identified with the occurrence of microbursts and other short duration precipitation bursts at this location [Rosenberg et al., 1971, 1981; Helliwell et al., 1980; Roeder et al., 1985]. Although the great majority of chorus bursts in this frequency range were composed of rising tones, there was the occasional falling tone. Note that the falling tone at 1131:01 UT on the Siple spectrogram of Figure 2 occurred at the time of a narrow

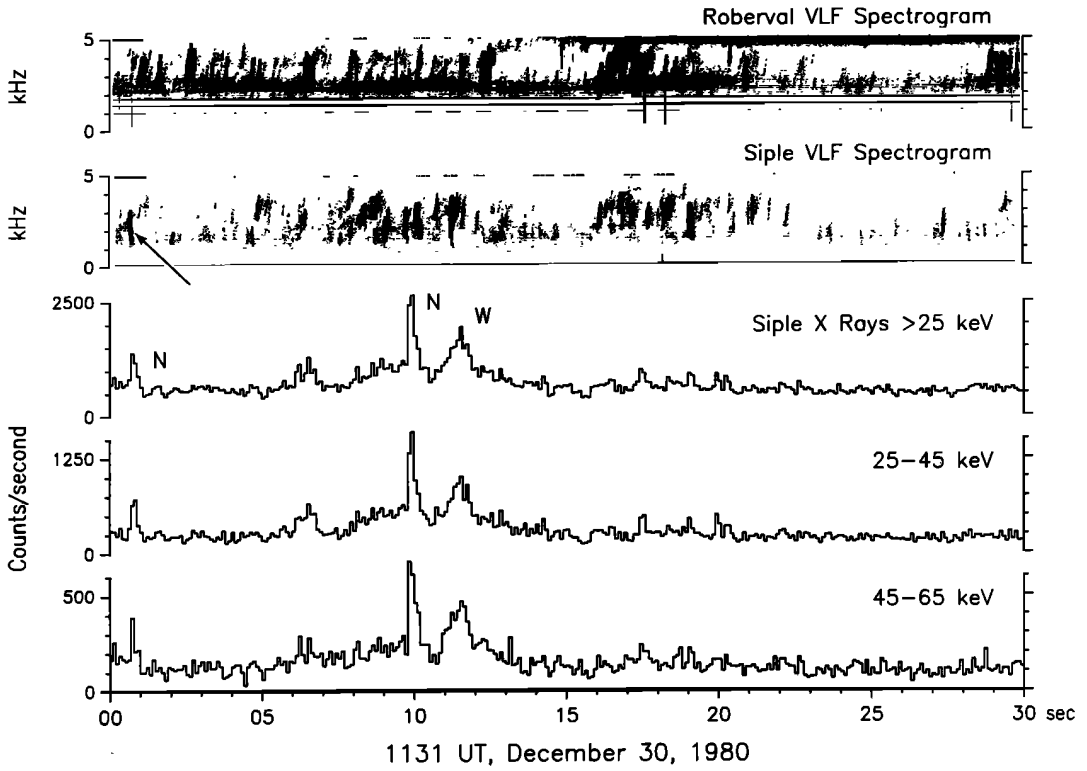

Fig. 2. Roberval and Siple 0-5 kHz VLF spectrograms and examples of highly resolved microbursts (0.1-s averages) recorded at Siple in the integral and first two differential energy channels of the X ray spectrometer. A distinction is made, as marked, between narrow (N) and wide (W) X ray bursts (see text for definitions). Chorus elements of rising frequency in the range ~ 2-4 kHz are the dominant emission evident in the spectrograms. The arrow denotes a falling tone in the Siple spectrogram that occurred at the time of a narrow microburst.

microburst. Such occurrences were extremely rare in the present data set.

Because of the complexity of the wave activity during most of the burst precipitation events on this day, it has not been possible to make unique identifications of individual correlated microbursts and chorus elements. This is frequently the case [e.g., Oliven and Gurnett, 1968; Rosenberg et al., 1981; Roeder et al., 1985]. Nevertheless, there is usually an interval during the recovery phase of a disturbed period when the precipitation and wave bursts are rather isolated,thus making the association between the two more readily apparent. This situation occurred for a short time near 1300 UT. At this time the X ray fluxes were down considerably from the higher levels observed earlier (see Figure 1), but continued to exhibit rapid temporal structure with burst groups separated by ~ 5-15 s, a range of spacings characteristic of pulsating aurora [Johnstone, 1978, 1983]. (Davidson [1986a,b] has shown that repetitive precipitation pulsations on this time scale can be viewed as a natural consequence of the feedback between wave growth and particle diffusion into the loss cone in a self-regulating process).

Two particularly good examples of the association of wave and particle bursts in the present data set are shown in Figure 3 which presents the Siple X ray counting rates in two energy channels ($E > 25$ keV and $45 < E \leq 65$ keV) and conjugate VLF data in the 0-5 kHz range. The associated events in each figure are highlighted by the short horizontal bars in each data panel. In (a) the Siple X ray and Roberval chorus bursts occur almost simultaneously and are of similar duration, whereas the Siple chorus burst begins ≥ 1 s earlier and has no obvious counterpart in either the X rays or the conjugate VLF. In (b) the Siple X ray and Roberval chorus bursts again occur almost simultaneously, but in this case the Siple chorus burst begins ≥ 1 s later. Even in these examples, however, we cannot uniquely identify a particular chorus element as the causative one responsible for a specific X ray enhancement within the overall precipitation burst.

In general, for the ~ 3-hr period examined in this paper, Siple X ray bursts appeared to be associated more closely with Roberval chorus bursts than with Siple chorus bursts as would be expected for the electron cyclotron resonance interaction [e.g., Rosenberg et al., 1981]. However, since readily identifiable correlations were rare in this data set, no further use is made of the VLF data.

Analysis

Microburst Event Selection

X ray microbursts were detected by an algorithm which scanned the $E > 25$ keV counting rate

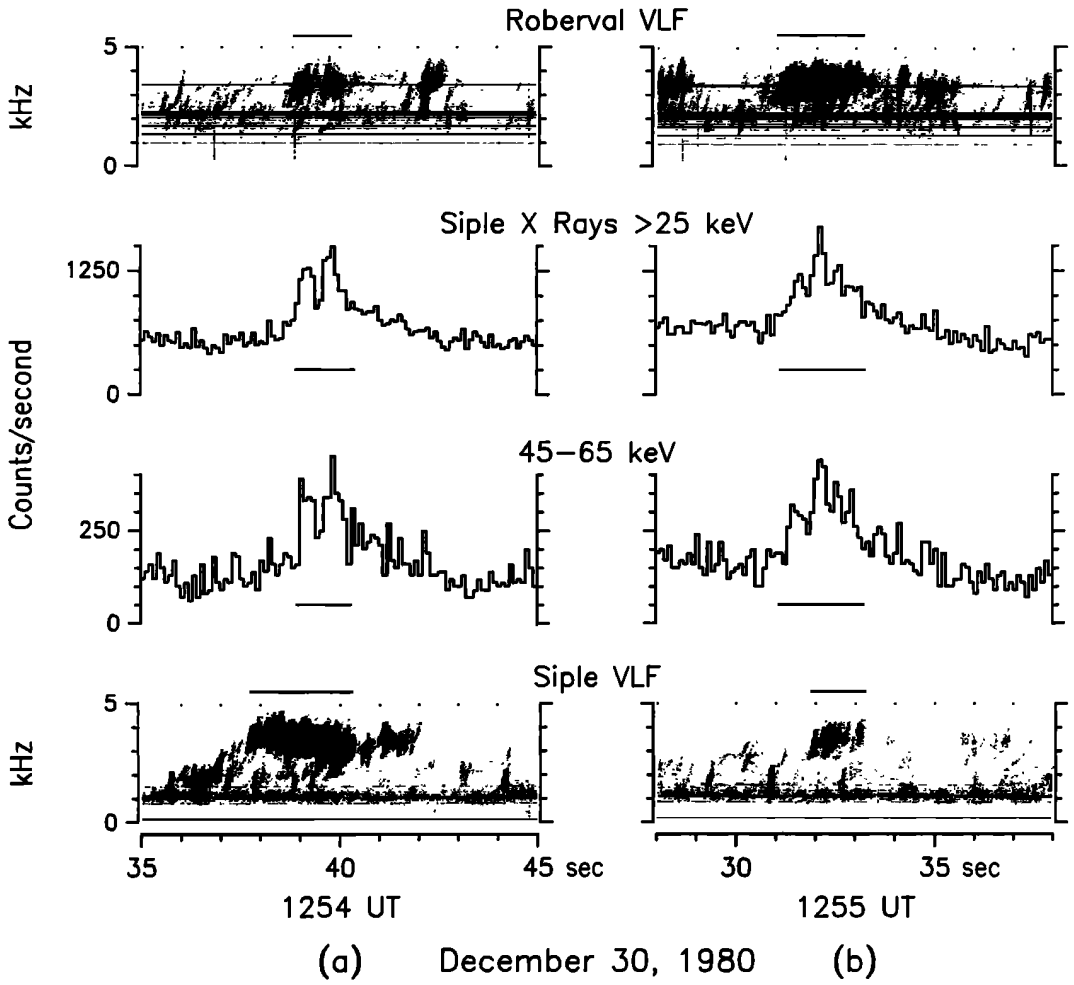

Fig. 3. Examples of the correlation of X ray microbursts and conjugate VLF emissions. Short horizontal bars indicate the approximate duration of associated events. In (a) the onsets of the Siple X ray and Roberval chorus bursts are approximately simultaneous, but are delayed by ~ 1 s from the onset of the Siple VLF burst; in (b) the onsets of the Siple X ray and Roberval chorus bursts are again simultaneous, but occur ~ 1 s prior to the onset of the Siple chorus burst.

time series and applied several criteria to distinguish microburst activity from other counting rate fluctuations. The algorithm was designed to detect single microbursts, with a time separation between events greater than about 1 s. However, because microbursts can occur in groups of two or more, with spacing on the order of a second or less, the program did not perform well in these regions of the time series; these microburst group events were culled from the initial selection. Inspection of plots of the events selected ensured that they satisfied the criteria established for the identification of single microburst events.

The events were found by examining the data in the integral channel, since this channel had the highest counting rate. The data were first averaged to 100 ms values from the 10 ms resolution of the instrument, and smoothed by applying a digital low-pass filter with a time constant of 100 ms. Since the mean counting rate varied considerably during the flight, a running mean, formed by a low pass filter with a 5-s time constant, was then subtracted from the 100 ms smoothed values. The resultant time series was then examined for events by scanning within a 4-s time interval, which was moved continuously along the time series.

The start of an event occurred when the counting rate exceeded a level above the running mean for 200 ms; this level was fixed arbitrarily at 10 times the square root of the running mean counting rate. The event ended when either the counting rate dropped below the starting level for 200 ms, or the event exceeded the end of the 4-s scanning interval, in which case it was discarded. The event candidate was also discarded if the peak counting rate did not exceed a level above the running mean of 25 times the square root of the mean. Scanning for the next event began 500 ms from the peak of the current event, so that multiple-peaked microbursts were not counted as separate events.

Distribution of Microburst Event Durations

The event selection technique described above detected 651 events in a 3-hr period during the

active part of the flight. The distribution of event durations for these 651 events is shown in Figure 4 which gives the percentage occurrence of microbursts as a function of width (defined as the full width at half-maximum counting rate). The distribution can be characterized as having a broad peak from 0.25 s to 0.6 s and a fairly rapid fall off above 0.6 s. A partitioning of the microbursts into two distinct categories, a narrow class (0.2-0.6 s) comprised of 452 events and a wide class (0.6-1.2 s) containing 199 events, is appropriate in view of the significantly smaller number of events having a duration > 0.6 s.

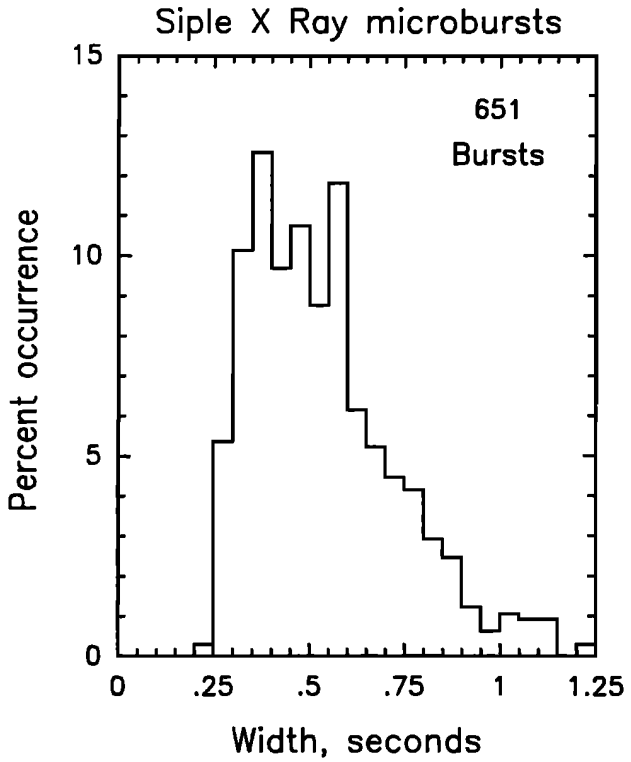

Fig. 4. Percentage distribution of X ray microbursts as a function of their full-width at half-maximum for 651 single, isolated bursts. Microbursts between 0.2 and 0.6 s width, approximately two thirds of the distribution, were designated narrow bursts in the subsequent analyses; those between 0.6 and 1.2 s were designated wide microbursts.

Microburst Energy Spectra and Fluxes

The properties of the average microburst in each category with respect to shape, duration, energy spectrum and flux were determined by a superposition analysis. The events were superposed in a 3-s interval centered on the time of maximum E > 25 keV counting rate.

The results of this analysis are presented in Figure 5a for the narrow distribution and in Figure 5b for the wide distribution. The top panel in each figure is the normalized counting rate profile for the E > 25 keV X ray channel. All events were normalized by subtracting the

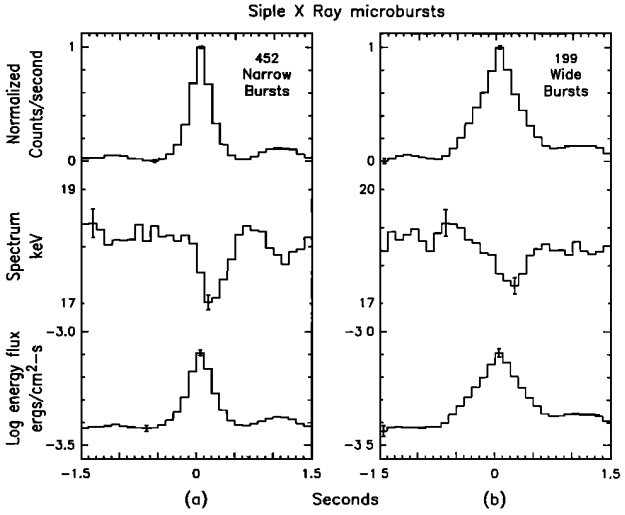

Fig. 5. Average profiles of X ray counting rate (E > 25 keV), energy spectrum (e-folding energy) and energy flux for (a) 452 narrow microbursts and (b) 199 wide microbursts superposed at the time (t = 0) of peak counting rate. The error bars indicated at the maximum and minimum values in each profile represent the standard deviation of the value at those times, divided by the square root of the number of microbursts superposed.

minimum counting rate during the superposition interval and dividing by the difference between the maximum and minimum counting rates. The half-length of the error bar is the standard deviation (calculated in the usual manner) divided by the square root of the number of events.

For both the wide and narrow distributions the average microburst is very nearly symmetric about the peak. For the narrow case the full width at half maximum of the average microburst is ~ 0.4 s, whereas for the wide case it is ~ 0.7 s. The symmetry of the distributions is essentially an artifact of the superposition method since, as we previously noted, individual bursts exhibit diverse temporal profiles with respect to their onset and recovery time constants. For most non-symmetric bursts, however, the difference between these time constants did not usually exceed 0.1-0.2 s. Consequently, although the superposition of either fast onset or fast recovery bursts would give somewhat narrower profiles than are shown in Figure 5, the distinction between narrow and wide bursts would still remain.

The middle panel in Figure 5 is a superposition of the X ray energy spectrum parameter computed for each microburst in the distributions. This parameter was estimated by fitting an exponential approximation to the counting rates of the three differential channels with energy limits of 25-45 keV, 45-65 keV, and 65-95 keV; it was not necessary to correct the counting rates for detector efficiency in this energy range. The higher energy differential channels were not used because the counting statistics were poor for many of the smaller microbursts. The uncertainty in individual estimates of the X ray energy spectrum parameter was of the order of 20%.

For both distributions in Figure 5 the microburst energy spectra were softer than the spectra that characterized the quasi-steady precipitation in the intervals between microbursts. The spectrum variation over the time interval encompassing the superposed microburst is consistent with the increasingly later arrival of lower energy electrons. The steepest part of the microburst spectrum followed the peak counting rate by ~ 0.1-0.2 s. On average, the change in the e-folding energy of the superposed X ray spectrum was of the order 1-3 keV. Individual microbursts exhibited a softening of the spectrum by as much as 5-10 keV in some instances. Energy spectrum variations within microbursts, similar to those found here, were also noted by Anderson and Milton [1964] to occur in some microburst episodes.

The X ray spectrum can be related to the incident electron spectrum using the results of Seltzer et al. [1973] and Berger and Seltzer [1972]. This involves comparing measured and calculated X ray spectra at a given atmospheric depth (8 g cm^{-2} in this case) assuming that the incident electron spectra can be approximated by exponential current distributions. For the range of X ray energy spectra encountered in this analysis (e-folding energies of ~ 15-20 keV), Table 4 of Berger and Seltzer [1972] shows that the X ray e-folding energy is about half the e-folding energy of the incident electrons. Table 1 gives the minimum and maximum e-folding energies for the X ray, and corresponding electron, spectra for superpositions of microbursts occurring at different times in the flight. As was pointed out earlier in connection with Figure 1, the tendency of the spectra to harden with time is evident. This spectrum hardening may have resulted in part from an increasingly harder quasi-steady enhanced precipitation. A narrow ELF frequency band at ~ 1 kHz also became more pronounced with time on the Siple records. Harder precipitation would be expected to arise from gyroresonant pitch angle scattering interactions of electrons with these lower frequency waves (than with the 2-4 kHz waves) for the same plasma conditions on the field line.

TABLE 1. e-Folding Energy Eo (keV) of Siple Microbursts

Time UT	X rays		Electrons	
	max	min	max	min
1053–1114	16.8	15.7	30.0	27.0
1114–1129	18.9	16.7	36.5	29.8
1129–1154	19.7	17.3	39.8	31.4
1154–1203	18.7	17.4	35.8	32.0
1203–1246	23.9	20.3	54.0	40.8
1053–1246	19.3	17.5	37.5	32.0

Finally, in Figure 5 the third panel gives the X ray energy flux (E > 0 keV) in erg cm^{-2} s^{-1} derived from the parameters of the least-square estimate of the spectrum of each microburst (i.e., the e-folding energy and counting rate extrapolated to zero energy). The energy flux profile for each microburst was not normalized, so that the superposition represents the mean energy flux for all the events included in the analysis. The peak X ray energy fluxes were ~ 10^{-3} erg cm^{-2} s^{-1}.

Computation of Chorus-Induced Precipitation

A test particle model of gyroresonant wave-induced pitch angle scattering in the magnetosphere [Inan et al., 1982; Chang and Inan, 1983a,b, 1985b; Chang et al., 1983] has been used to simulate chorus-induced microburst precipitation. The model is based on computing the trajectories of test particles that undergo cyclotron resonant encounters with the chorus waves at different points along the field line. In the context of this model, precipitation into, for example, the southern hemisphere may involve electrons that precipitate directly after being scattered by a north-going wave or those that are scattered by a south-going wave and that mirror in the conjugate hemisphere before precipitating in the south. These two categories are illustrated in Figures 2 and 6 of Chang and Inan [1983b] and are termed 'direct and 'mirrored' precipitation, respectively.

We have considered precipitation induced by a whistler-mode wave pulse of 0.2-s duration and having a linear frequency variation increasing from 2 to 4 keV. Such a wave pulse is representative of the individual discrete, rising tone emissions that were observed at Siple and Roberval during the microburst precipitation on this day and thus is an appropriate choice for studying energy-time features of chorus-induced microbursts.

The chorus signal was assumed to enter the magnetosphere at 1000 km altitude and to propagate from the southern (northern) to the northern (southern) hemisphere. Details of the propagation of the wave along the field line and its interaction with the distribution of trapped energetic electrons are given in the papers cited earlier in this section. It will suffice to point out that the wave magnetic field intensity at the magnetic equator was taken to be 10 pT at 2 kHz and the differential energy spectrum for trapped particles near the loss cone was taken to be $\phi(E) \sim \exp(-E/Eo)$ with $\Phi(E) = 10^6$ el $(cm^2\text{–s–sr–keV})^{-1}$ at E = 1 keV assumed as a typical level for the trapped electron flux. Calculations were performed for Eo values of 25, 50 and 100 keV and for equatorial cold plasma densities Neq of 10, 25 and 50 cm^{-3} on the L = 4.2 field line. Gaines et al. [1986] found that the spectrum of electrons from ~ 60 to 200 keV in the loss cone at low altitudes in the vicinity of Siple during weak-to-moderate precipitation can be characterized as exponential with Eo in the range ~ 20 to 100 keV. Equatorial cold plasma densities of 10-25 cm^{-3} are applicable to the present observations. This was inferred from the measurement of wave-echoing periods from analysis of simultaneous Siple and Roberval wave data.

Comparison of Observed and Calculated Microburst Features

The results of the calculations for both the direct and mirrored precipitation are shown in Figure 6 for the parameters Eo = 25 keV and Neq = 25 cm^{-3}. The top panels show the computed energy flux versus time and the bottom panels the energy range of the particles that constitute the flux. The reference time t = 0 is taken to be the time at which the wave packet enters the magnetosphere. For our purposes this choice has no effect on the analysis since no examination is made of time delays between microbursts and chorus. Our intent is only to compare the energy and temporal features of the observed microburst distributions with the model predictions of 'direct' and 'mirrored' precipitation.

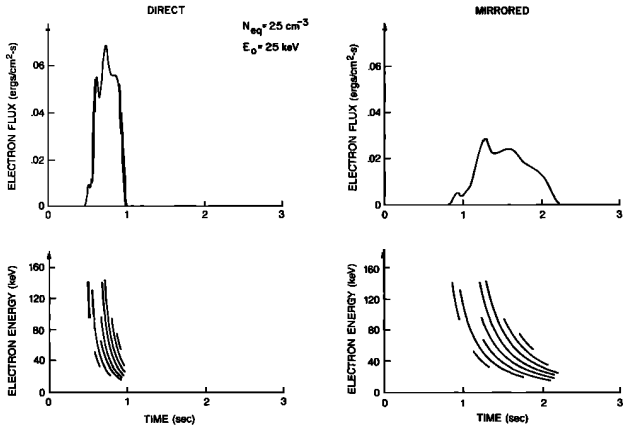

Fig. 6. Results of the test particle simulation showing energy flux profiles and electron energies contributing to the flux for direct precipitation (left hand panels) and mirrored precipitation (right hand panels). The calculations assumed an equatorial plasma density Neq of 25 cm^{-3} and a trapped electron spectrum with e-folding energy Eo of 25 keV.

Figure 6 shows that 1) the energy spectrum is hardest at the beginning of a burst; 2) the widths of the precipitated bursts are ≤ 0.5 s for the direct case, ≥ 0.5 s for the mirrored case; and 3) the peak precipitated energy flux in the mirrored case is approximately one-half that of the direct case. It is also to be noted that significant multiple-peaked structure (not shown) is predicted for the parameter range Eo ≥ 50 keV, Neq ≥ 25 cm^{-3}.

The main features of the calculated precipitated electron fluxes and burst durations are summarized in Table 2 for the full range of parameters considered in the calculations. For the direct case, we note that burst durations ranged from 0.23 to 0.44 s, whereas the corresponding range in the mirrored case was 0.40 to 0.95 s; the ratio of direct to mirrored fluxes varied from 1.8 to 2.9. For the parameters that apply to the present observations (Eo ≈ 25-50 keV, Neq ≈ 10-25 cm^{-3}), the average burst duration is ~ 0.3 s (direct) and ~ 0.7 s (mirrored), and the flux ratio is ~ 2.5.

TABLE 2. Computed Precipitated Electron Fluxes (ergs cm^{-2} s^{-1}) and Burst Durations T (seconds)

Eo (keV)	Neq=10 cm^{-3}		Neq=25 cm^{-3}		Neq=50 cm^{-3}	
	Flux	T	Flux	T	Flux	T
			Direct (D)			
25	0.047	0.23	0.068	0.35	0.075	0.35
50	0.20	0.28	0.23	0.33	0.20	0.44
100	0.66	0.23	0.50	0.30	0.51	0.38
			Mirrored (M)			
25	0.016	0.77	0.028	0.80	0.029	0.60
50	0.09	0.65	0.10	0.60	0.09	0.95
100	0.29	0.40	0.22	0.67	0.28	0.74
			Flux Ratio, D/M			
25	2.9		2.4		2.6	
50	2.2		2.3		2.2	
100	2.3		2.3		1.8	

The test particle model calculations carried out in this paper for the interpretation of the December 30, 1980 data are in many ways similar to the analysis by Chang and Inan [1983b] of another case of short-duration X ray bursts observed at Siple station, Antarctica [Rosenberg et al., 1971]. The individual discrete chorus elements were not as well defined in those data and there was not sufficient energy or time resolution with which to examine the energy or time evolution of the X ray bursts. Chang and Inan considered a power-law trapped electron energy distribution with a similar range of cold plasma densities as was used here. However, the previous work only addressed the mirrored precipitation case and the duration of the chorus burst (frequencies varying from 2 to 4 kHz, as is the case here) was taken to be 0.5 s rather than the 0.2 s used in the present study. The frequency ramp used in the present calculation is believed to be a more realistic representation of the chorus waves that produced the scattering on December 30, 1980.

Summary and Conclusions

Energy-time features of X ray microbursts observed at Siple station, Antarctica (L ~ 4.2) have been compared with computer simulations of the burst precipitation of trapped energetic electrons in cyclotron resonance with VLF chorus.

Two categories of microbursts were suggested by the distribution of burst durations; narrow microbursts of 0.2-0.6 s duration comprising approximately two-thirds of the distribution (of 651 events analyzed) and wide microbursts of 0.6-1.2 s duration. For both categories the precipitated energy spectrum was softest near the peak of the energy influx. Assuming an exponential electron energy distribution the spectral softening was ≤ 5 keV e-folding energy; the quasi-steady precipitation that occurred between bursts was characterized by electron spectra of

the order 25-50 keV e-folding energy during the ~ 3-hr interval of microburst activity.

Test particle computer simulations of precipitation induced by gyroresonant wave-particle interactions were applied to consider two cases: 1) direct precipitation, whereby electrons after undergoing pitch-angle scattering by the wave pulse precipitate directly into the ionosphere; and 2) mirrored precipitation, whereby the scattered electrons first mirror above the conjugate ionosphere before precipitating at the opposite end of the field line. The calculations were performed for a range of plasma, energetic particle, and wave parameters appropriate to the observational conditions. The features imparted to precipitated electron pulses by the wave-particle interaction and the particle travel time from a near-equatorial interaction region compare favorably with the observed microburst durations and energy spectrum variations. The main points of this comparison are as follows:

1. A combined effect of energy dispersion and latitude dependence of the energy of maximum gyroresonant scattering leads to a softening of the energy spectrum of the precipitated pulse, in qualitative agreement with the observations.

2. The average ratio of direct-to-mirrored peak energy fluxes of ~ 2.5 is in quantitative agreement with the observed ratio of peak fluxes of narrow and wide microbursts of ~ 2.

3. Some examples of multiple-peaked microbursts were seen in the data. The computer simulations show that such bursts can occur if Eo $\approx$ 50 keV and Neq $\approx$ 25 cm^{-3} for the wave pulse assumed. These values of Eo and Neq are believed to be near the limit of the parameter range for the activity on this day.

4. Finally, the calculated burst durations of 0.2-0.5 s and 0.5-1.0 s for the direct and mirrored precipitation pulses span the observed distribution of microburst durations. We suggest on this basis that narrow (wide) microbursts be identified with direct (mirrored) precipitation.

The present results (i.e., mirrored burst durations, spectrum softening, multiple-peaked structure) are consistent with the results of Chang and Inan [1983b] applied to an earlier case [Rosenberg et al., 1971] of wave-induced electron precipitation bursts. These findings provide further support for the belief that microbursts can arise in the type of gyroresonance process that is modeled in the work of Inan et al. [1982] and related papers. Further experimental and theoretical studies are needed in order to extend our knowledge of burst precipitation and to refine our theoretical understanding and modeling of its origins.

Acknowledgments. This work was supported by the Division of Polar Programs of the National Science Foundation under grants DPP 8217260 and DPP 8614457 to the University of Maryland and grants DPP 8217820 and DPP 8317092 to Stanford University. We gratefully acknowledge the assistance of personnel from the University of Maryland, the University of Houston and Stanford University who participated in the balloon launch operations and related data-gathering activities at Siple station and Roberval. Useful discussions were held with R. A. Helliwell, D. L. Carpenter and D. L. Matthews. We thank B. Casanova for preparing the typescript.

The Editor thanks N. Cornilleau-Wehrlin, G. T. Davidson and a third referee for their assistance in evaluating this paper.

References

Anderson, K. A., and D. W. Milton, Balloon observations of X rays in the auroral zone, 3. High time resolution studies, J. Geophys. Res., 69, 4457-4470, 1964.

Berger, M. J., and S. M. Seltzer, J. Atmos. Terr. Phys., 34, 85-108, 1972.

Bering, E. A., T. J. Rosenberg, J. R. Benbrook, D. Detrick, D. L. Matthews, M. J. Rycroft, M. A. Saunders, and W. R. Sheldon, Electric fields, electron precipitation and VLF radiation during a simultaneous magnetospheric substorm and atmospheric thunderstorm, J. Geophys. Res., 85, 55, 1980.

Chang, H. C., and U. S. Inan, Quasi-relativistic electron precipitation due to interactions with coherent VLF waves in the magnetosphere, J. Geophys. Res., 88, 318, 1983a.

Chang, H. C., and U. S. Inan, A theoretical model study of observed correlations between whistler mode waves and energetic electron precipitation events in the magnetosphere, J. Geophys. Res., 88, 10,053-10,058, 1983b.

Chang, H. C., and U. S. Inan, Lightning-induced electron precipitation from the magnetosphere, J. Geophys. Res., 90, 1531, 1985a.

Chang, H. C., and U. S. Inan, Test particle modeling of wave-induced energetic electron precipitation, J. Geophys. Res., 90, 6049, 1985b.

Chang, H. C., U. S. Inan and T. F. Bell, Energetic electron precipitation due to gyroresonant interactions in the magnetosphere involving coherent VLF waves with slowly varying frequency, J. Geophys. Res., 88, 7037, 1983.

Davidson, G. T., Pitch angle diffusion in morningside aurorae. 1. The role of the loss cone in the formation of impulsive bursts of precipitation, J. Geophys. Res., 91, 4413, 1986a.

Davidson, G. T., Pitch angle diffusion in morning-side aurorae. 2. The formation of repetitive pulsations, J. Geophys. Res., 91, 4429, 1986b.

Foster, J. C., and T. J. Rosenberg, Electron precipitation and VLF emissions associated with cyclotron resonance interactions near the plasmapause, J. Geophys. Res., 81, 2183, 1976.

Gaines, E. E., W. L. Imhof, W. E. Francis, M. Walt and T. J. Rosenberg, Correlated electron and X ray measurements of quiet time electron precipitation: A comparative study of bremsstrahlung production and transport in the atmosphere, J. Geophys. Res., 91, 13, 455, 1986.

Goldberg, R. A., J. R. Barcus, L. C. Hale, and S. A. Curtis, Direct observation of magnetospheric electron precipitation stimulated by lightning, J. Atmos. Terr. Phys., 48, 293, 1986.

Haugstad, B. S., and T. Pytte, Effects of primary electron transit times on power spectra of auroral-zone X ray microbursts, J. Atmos. Terr. Phys., 39, 689, 1977.

Helliwell, R. A., J. P. Katsufrakis, and M. L. Trimpi, Whistler-induced amplitude perturbation in VLF propagation, J. Geophys. Res., 78, 4679, 1973.

Helliwell, R. A., S. B. Mende, J. H. Doolittle, W. C. Armstrong and D. L. Carpenter, Correlations between λ4278 optical emissions and VLF wave events observed at L ~ 4 in the Antarctic, J. Geophys. Res., 85, 3376, 1980.

Imhof, W. L., J. B. Reagan, H. D. Voss, E. E. Gaines, D. W. Datlowe, J. Mobilia, R. A. Helliwell, U. S. Inan, and J. Katsufrakis, The modulated precipitation of radiation belt electrons by controlled signals from VLF transmitters, Geophys. Res. Lett., 10, 615, 1983.

Inan, U. S., T. F. Bell, and R. A. Helliwell, Non-linear pitch angle scattering of energetic electrons by coherent VLF waves in the magnetosphere, J. Geophys. Res., 83, 3235, 1978.

Inan, U. S., T. F. Bell, and H. C. Chang, Particle precipitation induced by short-duration VLF waves in the magnetosphere, J. Geophys. Res., 87, 6243, 1982.

Inan, U. S., D. L. Carpenter, R. A. Helliwell, and J. P. Katsufrakis, Subionospheric VLF/LF phase perturbations produced by lightning-whistler induced particle precipitation, J. Geophys. Res., 90, 7457, 1985.

Johnstone, A. D., Pulsating aurora, Nature, 274, 119, 1978.

Johnstone, A. D., The mechanism of pulsating aurora, Ann. Geophys., 1, 397, 1983.

Kennel, C. F., and H. E. Petschek, Limit on stably trapped particle fluxes, J. Geophys. Res., 71, 1, 1966.

Khrustchinsky, A. A., I. A. Kornilov, L. L. Lazutin, and W. Riedler, On the location of the source for X ray microbursts, Proc. Conf. Achievements of the IMS, 26-28 June 1984, Graz, Austria ESA SP-217, 325-327, 1984.

Lampton, M., Daytime observations of energetic auroral-zone electrons, J. Geophys. Res., 72, 5817, 1967.

Lazutin, L. L., X ray Emission of Auroral Electrons and Magnetospheric Dynamics, Springer-Verlag, 1986.

Oliven, M. N., and D. A. Gurnett, Microburst phenomena, 3, An association between microbursts and VLF chorus, J. Geophys. Res., 73, 2355, 1968.

Parks, G. K., Auroral zone microbursts, substructures and a model for microburst precipitation, Proc. Int. Conf. X rays Space (Cosmic, Solar, Auroral X rays), 2, 849-874, 1975.

Parks, G. K., Microburst precipitation phenomena, J. Geomagn. Geoelectr., 30, 327, 1978.

Roeder, J. L., J. R. Benbrook, E. A. Bering, III, and W. R. Sheldon, X ray microbursts and VLF chorus, J. Geophys. Res., 90, 10,975-10,982, 1985.

Rosenberg, T. J., R. A. Helliwell, and J. P. Katsufrakis, Electron precipitation associated with discrete very low frequency emissions, J. Geophys. Res., 76, 8445, 1971.

Rosenberg, T. J., J. C. Siren, D. L. Matthews, K. Marthinsen, J. A. Holtet, A. Egeland, D. L. Carpenter, and R. A. Helliwell, Conjugacy of electron microbursts and VLF chorus, J. Geophys. Res., 76, 5819-5832, 1981.

Seltzer, S. M., M. J. Berger, and T. J. Rosenberg, Auroral bremsstrahlung at balloon altitudes, NASA SP-3081, 1973.

Voss, H. D., W. L. Imhof, M. Walt, J. Mobilia, E. E. Gaines, J. B. Reagan, U. S. Inan, R. A. Helliwell, D. L. Carpenter, J. P. Katsufrakis, and H. C. Chang, Lightning-induced electron precipitation, Nature, 312, 740, 1984.

D. L. Detrick and T. J. Rosenberg, Institute for Physical Science and Technology, University of Maryland, College Park, MD 20742.

U. S. Inan, Space, Telecommunications and Radioscience Laboratory, Stanford University, Stanford, CA 94305.

R. Wei, Institute of Space Physics, Chinese Academy of Sciences, P.O. Box 5112, Beijing, China.

(Received April 14, 1987;
revised January 8, 1990;
accepted January 8, 1990.)